Progress In Electromagnetics Research C, Vol. 124, 33–42, 2022

A Novel Method for Rapidly Solving Wideband RCS by Combining UCBFM and Compressive Sensing

Zhonggen Wang[1], Chenwei Li[1, *], Yufa Sun[2], Wenyan Nie[3], Pan Wang[1], and Han Lin[1]

Abstract—While analyzing wideband electromagnetic scattering problems using ultra-wideband characteristic basis function method (UCBFM), the reconstruction of a reduced matrix and the recalculation of an impedance matrix at each frequency point cost a large amount of time. To overcome this issue, a novel method that combines UCBFM with compressive sensing (CS) is proposed in this paper to rapidly analyse the wideband RCS. The proposed method makes the ultra-wideband characteristic basis functions (UCBFs) generated at the highest frequency as the sparse basis, introduces the CS theory, randomly extracts several rows from the original matrix as the measurement matrix, utilizes the corresponding excitation vector as the measurement value, and then employs the recovery algorithm, through which the solution of target induced current can be obtained. Due to partial filling of impedance matrix and efficient recovery algorithm, the wideband RCS computation time of the object is significantly reduced using the proposed method. Furthermore, the numerical simulation results show that the computation efficiency for the target wideband RCS can be further enhanced compared with that of the stand-alone UCBFM.

1. INTRODUCTION

The traditional method of moments (MoM) [1] can be applied for the accurate solution of wideband electromagnetic (EM) scattering problems. However, the impedance matrix filled by MoM is essentially a dense matrix, and as the target size increases, the impedance matrix expands rapidly, thereby heavily burdening the computer's memory and CPU calculations. Likewise, many efficient acceleration algorithms have been proposed to solve this problem. Among them, one approach is to reduce the complexity of the matrix-vector product, such as the adaptive cross approximation (ACA) algorithm [2], fast dipole method (FDM) [3], and adaptive integration method (AIM) [4]. Yet another technique is to introduce macro basis functions to reduce the dimensions of a MoM matrix, such as synthetic basis function (SBF) method [5] and characteristic basis function method (CBFM) [6–8]. Although these methods improve the computational efficiency of the MoM in solving electrically large objects at a single frequency point, the overall efficiency eventually becomes low, since the calculation process has to be repeated for each frequency point over the whole frequency band. The interpolation techniques have been proposed to alleviate this problem, including the model-based parameter estimation (MBPE) [9], impedance interpolation technology [10], and asymptotic waveform evaluation (AWE) technology [11], but these methods are all iterative methods. In order to address the above issue, an effective ultra-wideband characteristic basis function method (UCBFM) [12, 13] has been developed to calculate the wideband radar cross section (RCS). This approach takes the characteristic basis functions (CBFs)

Received 21 July 2022, Accepted 29 August 2022, Scheduled 11 September 2022

* Corresponding author: Chenwei Li (cwli17355488791@163.com).

[1] School of Electrical and Information Engineering, Anhui University of Science and Technology, Huainan 232001, China. [2] Key Lab of Intelligent Computing & Signal Processing, Anhui University, Hefei 230039, China. [3] School of Mechanical and Electrical Engineering, Huainan Normal University, Huainan 232001, China.

at the highest frequency point, after the singular value decomposition (SVD) procedure, as the ultra-wideband CBFs (UCBFs). Since these UCBFs can reflect the current waveform characteristics of a wider frequency band, they can be effectively reused over the entire frequency band. However, it should be noted that the number of UCBFs in such a case is higher than necessary, and the computational complexity will be increased when applying the UCBFs to lower frequency points. Besides, the reduced matrix equation and the impedance matrix for each frequency point also need to be recalculated. Therefore, over the recent years, many improved UCBFM methods have been proposed in literature to enhance its performance for wideband scattering problems. In [14], an algorithm that amalgamates UCBFM with an adaptive technique has been presented, for calculating the wideband RCS data, which can reduce the number of UCBFs at lower sub-frequency band data. In [15, 16], the MBPE and AWE technologies are respectively combined with the UCBFM for the fast evaluation of wideband RCS data, which improve the computational efficiency by reducing the number of frequency points that need to be calculated. Unfortunately, none of these reported approaches can speed up the filling of the impedance matrix at each frequency point, when calculating the wideband RCS.

In this paper, a new method combining compressive sensing (CS) [17–19] and UCBFM (CS-UCBFM) is proposed to overcome the above-mentioned challenges in efficiently analyzing the wideband RCS. In the proposed CS-UCBFM, the UCBFs constructed at the highest frequency point are utilized as the sparse basis. The impedance matrix randomly drawn by the compressive sensing acts as the measurement matrix, and the corresponding excitation vector serves as the measured value. Then, an efficient reconstruction of current coefficients can be realized using least square method [20]. Finally, numerical simulations for differently shaped objects are presented to validate the accuracy and efficiency of the proposed method.

2. FORMULATION

2.1. Construction of UCBFs

The UCBFM first divides the target into M blocks, where each block is extended for avoiding the singular behaviour in the current distribution. Then, by modeling at the highest frequency point f_h of the frequency band, each block is characterized through a set of primary CBFs (PCBFs). Finally, incident plane waves are set uniformly according to $\Delta\theta$ and $\Delta\Phi$ above each block, and considering two polarization modes, a total of $N_{\mathrm{PWS}} = 2N_\theta N_\varphi$ incident waves are required, denoted as $\mathbf{E}_i^{N_{\mathrm{PWS}}}h$. Here, $N_\theta N_\theta$, N_φ represent the number of incident plane waves in θ and φ directions, respectively. Assuming that the number of Rao-Wilton-Glisson (RWG) vector basis functions of each extended block is N_i, the PCBFs of the ith block can be solved by the following formula:

$$\mathbf{Z}_{ii}(f_h) \cdot \mathbf{J}_i^{\mathrm{CBF}}(f_h) = \mathbf{E}_i^{N_{\mathrm{PWS}}}(f_h) \tag{1}$$

where $\mathbf{Z}_{ii}(f_h)$ is the self-impedance matrix of block i with size $N_i \times N_i$; $\mathbf{E}_i^{N_{\mathrm{PWS}}}(f_h)$ is the $N_i \times N_{\mathrm{PWS}}$ matrix containing excitation vectors; and $\mathbf{J}_i^{\mathrm{CBF}}(f_h)$ is the $N_i \times N_{\mathrm{PWS}}$ matrix to be obtained, which contains the PCBFs of block i. Since $\mathbf{J}_i^{\mathrm{CBF}}(f_h)$ corresponds to the PCBFs generated by multiple excitations, it contains a lot of redundant information. Next, a new set of basis functions that are linear combinations of original PCBFs is constructed via the SVD approach, and only the functions with relative singular values above a certain threshold, for example, 10E-3, are retained. These remaining PCBFs for each block after the SVD processing are named as UCBFs ($\mathbf{J}_i^{\mathrm{UCBF}}(f_h)$). For simplicity, we assume that all blocks contain the same number of K UCBFs after the SVD, and then, the current of target at any frequency point f can be expressed as

$$\mathbf{J}(f) = \sum_{i=1}^{M}\sum_{k=1}^{K} \alpha_i^k(f)\mathbf{J}_i^{\mathrm{UCBF}_k}(f_h) \tag{2}$$

where $\mathbf{J}_i^{\mathrm{UCBF}_k}(f_h)$ represents the kth UCBFs of block i, and $\alpha_i^k(f)$ refers to the unknown weighting coefficients to be calculated for frequency f. Moreover, the $\alpha_i^k(f)$ for any frequency point can be obtained by solving the reduced matrix equation, given as

$$\mathbf{Z}^{\mathrm{R}}(f) \cdot \alpha(f) = \mathbf{E}^{\mathrm{R}}(f) \tag{3}$$

where the elements of $\mathbf{Z}^{\mathrm{R}}(f)$, $\mathbf{E}^{\mathrm{R}}(f)$ are constructed using the following equation:

$$Z_{ij}^{\mathrm{R}}(f) = \mathbf{J}_i^{\mathrm{UCBF^T}}(f_h) \cdot \mathbf{Z}_{ij}(f) \cdot \mathbf{J}_j^{\mathrm{UCBF}}(f_h) \tag{4}$$

$$E_i^{\mathrm{R}}(f) = \mathbf{J}_i^{\mathrm{UCBF^T}}(f_h) \cdot \mathbf{E}_i(f) \tag{5}$$

where T represents the transpose operation. Since $\mathbf{J}_i^{\mathrm{UCBF}}(f_h)$ contains adequate current waveform characteristics over the entire frequency band, it can be reused for any frequency point in the construction of $Z_{ij}^{\mathrm{R}}(f)$ and $E_i^{\mathrm{R}}(f)$, thus reducing the CBFs construction time. However, the reduced matrix Equation (4) needs to be repeatedly constructed at each frequency point, wherein the calculation of impedance matrix ($\mathbf{Z}_{ij}(f)$) requires a significant amount of computing time, when large objects with small frequency steps are analyzed.

2.2. UCBFs as Sparse Basis to Construct Underdetermined Equation

To solve EM scattering problems, the MoM is used to convert the integral equation into an impedance matrix equation as

$$\mathbf{Z}(f_x)\mathbf{I}(f_x) = \mathbf{V}(f_x) \tag{6}$$

where f_x is the incident wave frequency, $\mathbf{Z}(f_x)$ the impedance matrix, $\mathbf{V}(f_x)$ the excitation vector, and $\mathbf{I}(f_x)$ the current vector to be found. While analyzing wideband scattering problems of the target, by introducing UCBFs, the above (6) can be changed to:

$$\mathbf{Z}_{N\times N}(f_x)\mathbf{J}_{N\times MK}(f_h)\alpha_{MK\times 1}(f_x) = \mathbf{V}_{N\times 1}(f_x) \tag{7}$$

where $\mathbf{Z}_{N\times N}(f_x)$, $\mathbf{V}_{N\times 1}(f_x)$, $\alpha_{MK\times 1}(f_x)$ represent the impedance matrix, excitation vector, and weighting coefficients matrix to be determined at the xth frequency point, respectively. Meanwhile, N is the number of RWG basis functions, and MK is the total number of UCBFs.

To enhance the computational efficiency of UCBFM, the CS theory commonly used in signal processing is introduced into Equation (7), to accelerate the filling of impedance matrix at each frequency point and reduce the current solution time. Firstly, by extracting only p rows of the impedance matrix and corresponding excitations, an underdetermined equation is constructed:

$$\widetilde{\mathbf{Z}}_{p\times N}(f_x)\mathbf{J}_{N\times MK}(f_h)\alpha_{MK\times 1}(f_x) = \widetilde{\mathbf{V}}_{p\times 1}(f_x) \tag{8}$$

where $\widetilde{\mathbf{Z}}_{p\times N}(f_x)$ denotes the measurement matrix, and $\widetilde{\mathbf{V}}_{p\times 1}(f_x)$ is considered as the measured value. In (8), $\mathbf{J}_{N\times MK}(f_x)$ can be regarded as the sparse transform matrix, and $\alpha_{MK\times 1}(f_x)$ denotes the weighting coefficients to be recovered. Utilizing the CS theory, the recovery matrix $\mathbf{\Theta}$ is then obtained as follows:

$$\mathbf{\Theta}_{p\times MK} = \widetilde{\mathbf{Z}}_{p\times N}(f_x)\mathbf{J}_{N\times MK}(f_h) \tag{9}$$

By substituting (9) into (8), Equation (8) can then be rewritten as

$$\widetilde{\mathbf{V}}_{p\times 1}(f_x) = \widetilde{\mathbf{Z}}_{p\times N}(f_x)\mathbf{J}_{N\times MK}(f_h)\alpha_{MK\times 1}(f_x) = \mathbf{\Theta}_{p\times MK}\alpha_{MK\times 1}(f_x) \tag{10}$$

Finally, since the number of UCBFs MK is smaller than the available number of rows p extracted from the impedance matrix, an efficient optimization algorithm (least square method) is applied to reconstruct the $\alpha_{MK\times 1}(f_x)$, and then, (10) can be solved in the least square sense as

$$\widehat{\alpha}_{MK\times 1}(f_x) = \left(\mathbf{\Theta}_{p\times MK}^{\mathbf{T}}\mathbf{\Theta}_{p\times MK}\right)^{-1}\left(\mathbf{\Theta}_{p\times MK}^{\mathbf{T}}\widetilde{\mathbf{V}}_{p\times 1}(f_x)\right) \tag{11}$$

where vector $\widehat{\alpha}_{MK\times 1}(f_x)$ is the solution of the optimization problem. Compared with the UCBFM, the CS-UCBFM reduces the calculation time for a single frequency point by decreasing the dimensions of impedance matrix filling, and speeds up the single frequency point RCS calculation, which effectively improves the calculation efficiency for the whole wideband RCS.

3. COMPLEXITY ANALYSIS

The calculation process of UCBFM and CS-UCBFM mainly includes three steps: the construction of UCBFs, the filling of impedance matrix, and the solution process of RCS. Since the first step is common in both methods, in this section we only compare the complexity of other two steps.

Filling impedance matrix: In UCBFM, the complexity of this step is $O(M^2N_i^2)$, where N_i is the number of unknowns of each block after the expansion. On the other hand, since the mutual impedance matrix is filled with only p rows in CS-UCBFM, the corresponding complexity is $O(pN)$, where N represents the total number of unknowns before dividing the blocks. Since $p < MN_i$ and $N < MN_i$, CS-UCBFM has a remarkable advantage over UCBFM.

RCS solution process: In UCBFM, the construction of reduced matrix and the solution of reduced matrix equation are the two main steps in solving the current, whose combined complexity is $O(M^2K^2N_i^2 + (KM)^3)$. Similarly, in CS-UCBFM, the RCS solution step contains the construction of recovery matrix and the solution of equation (11), and the corresponding complexity is $O(pNKM + M^2K^2p + M^2K^2 + MKp) \approx O(pNKM + M^2K^2p)$. Considering $pNKM < M^2K^2N_i^2$, the RCS solution time with CS-UCBFM will be shorter than that with UCBFM.

From the above analysis, it can be concluded that the calculation cost can be decreased dramatically by using CS-UCBFM.

4. NUMERICAL RESULTS

To validate the efficiency and accuracy of the proposed method, the wideband RCS of three differently shaped perfect electrical conductor (PEC) objects is calculated in this section. All the numerical results are computed on a personal computer with Intel (R) Core (TM) i5-6500 CPU with 3.20 GHz and 32 GB RAM. In addition, the SVD threshold for all cases is 0.001, and a total of 800 plane waves are set to generate the CBFs. In this paper, relative root mean square error (RRMSE) function is referenced to analyze the error in the calculation results of wideband RCS, which is defined as

$$\text{RRMSE} = \sqrt{\sum_{i=1}^{n} (X_{cal,i} - X_{ref,i})^2} \Bigg/ \sqrt{\sum_{i=1}^{n} X_{ref,i}^2} \tag{12}$$

where $X_{cal,i}$ represents the RCS value calculated by UCBFM or CS-UCBFM, $X_{ref,i}$ the reference results calculated using commercial software FEKO, and n the number of frequency points to be solved in the corresponding frequency band.

4.0.1. PEC Cube

First, the wideband RCS of a PEC cube in the 0.6G to 3G frequency band is calculated, where the side length of the cube is 0.18 m. Moreover, the target is meshed at the highest frequency point, resulting in a total of 7410 triangular patches and 11115 unknowns. Next, the target is divided into 8 blocks, and each block is extend by 0.15λ. Here, a total of 15159 unknowns are generated, and 1004 UCBFs are obtained. In order to demonstrate the feasibility of using UCBFs as sparse basis in the CS-UCBFM, the sparseness of the induced current on discrete cosine transform (DCT) sparse basis and UCBFs sparse basis is compared, as shown in Figs. 1 and 2, respectively. Obviously, there are too many non-zero elements in Fig. 1, indicating that the induced currents are not sparse on the DCT domain. On the contrary, the amplitude of induced currents on UCBFs sparse basis shows a fine sparseness (Fig. 2), where most of the values are zero or close to zero, while only a few non-zero values play a dominant role.

After verifying that UCBFs can be used as sparse bases, a suitable value for the extraction ratio in CS-UCBFM also needs to be decided. The relationship between the extraction ratio p/N and the RCS error is illustrated in Fig. 3. It can be seen that as the value of p/N increases above 0.3, the RCS error fluctuates continuously in the range of 0 to 1 with small increments; however, the computation time will increase continuously with the increase of extraction ratio. In order to balance the accuracy and time cost, the value of p/N is set between 0.3 and 0.5. In order to prove the calculation stability

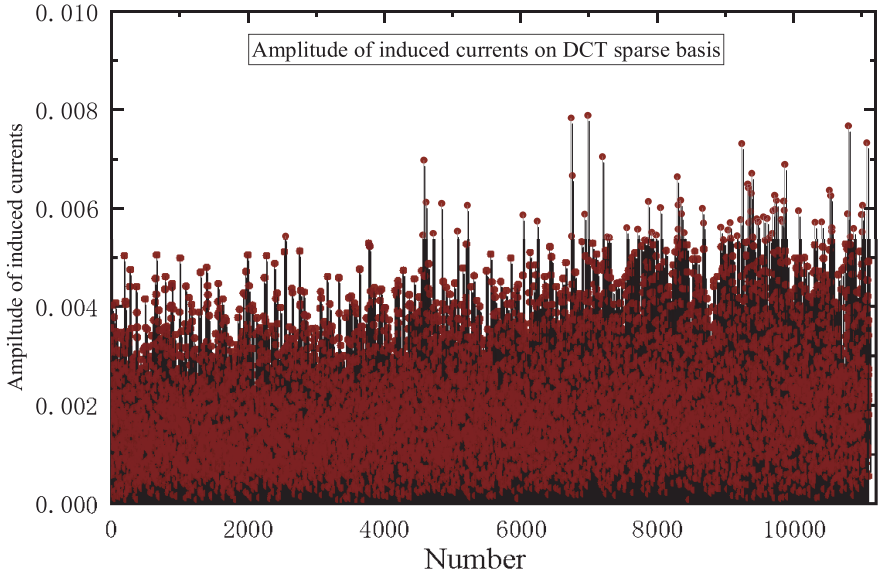

Figure 1. Amplitude of induced currents on DCT sparse basis.

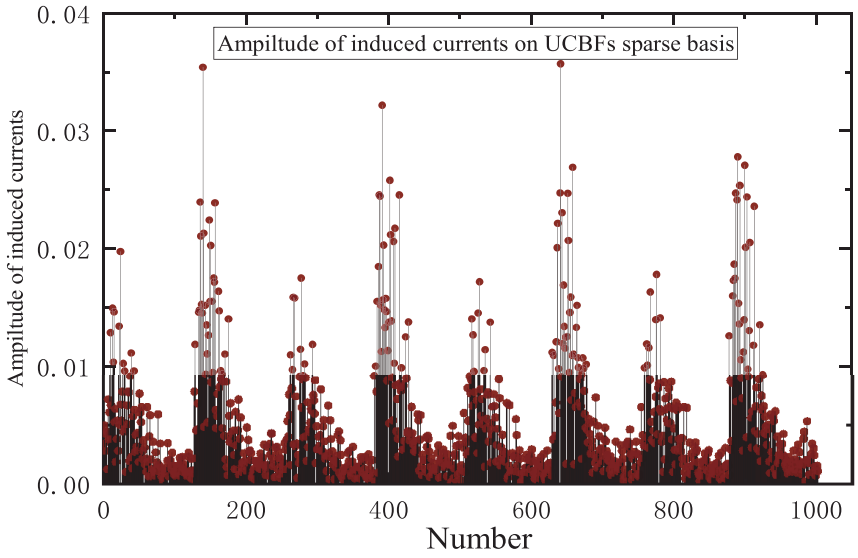

Figure 2. Amplitude of induced currents on UCBFs sparse basis.

of random extraction method, Fig. 4 gives the RCS error distribution of 5000 extraction experiments using CS-UCBFM. It can be seen from Fig. 4 that when random extraction method is adopted, the RCS error fluctuates within a small range, and the calculation results are stable. In the case of $p/N = 0.3$, the wideband RCS patterns for 21 frequency points of the cube in vertical polarization are plotted in Fig. 5. It can be seen from the figure that the results calculated by CS-UCBFM are in good agreement with UCBFM.

4.1. PEC Sphere

Additionally, the EM scattering characteristics of a PEC sphere in the frequency band from 1G to 2G are also analyzed, where the radius of the sphere is 0.225 m. The geometry is discretized into 10328 triangles resulting in 15492 unknowns, and then divided into 8 blocks, where each block is extended

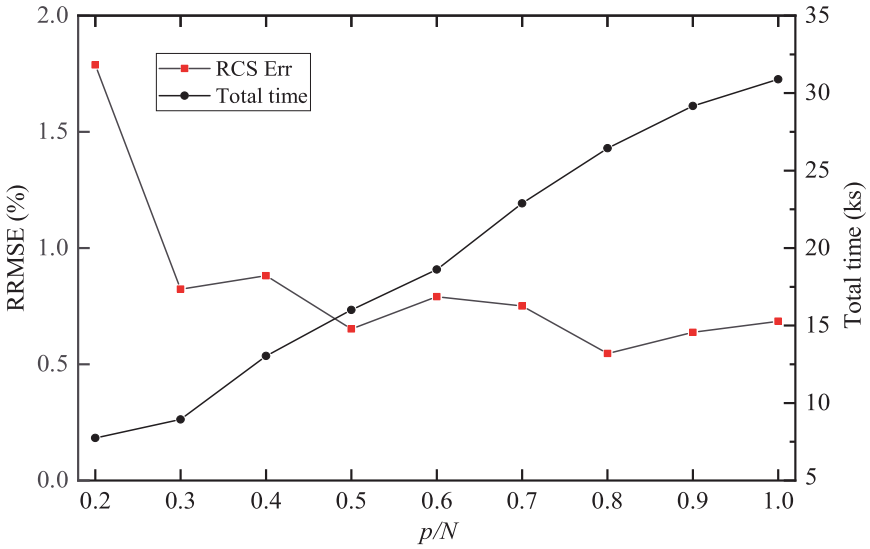

Figure 3. RCS Err against p/N for CS-UCBFM.

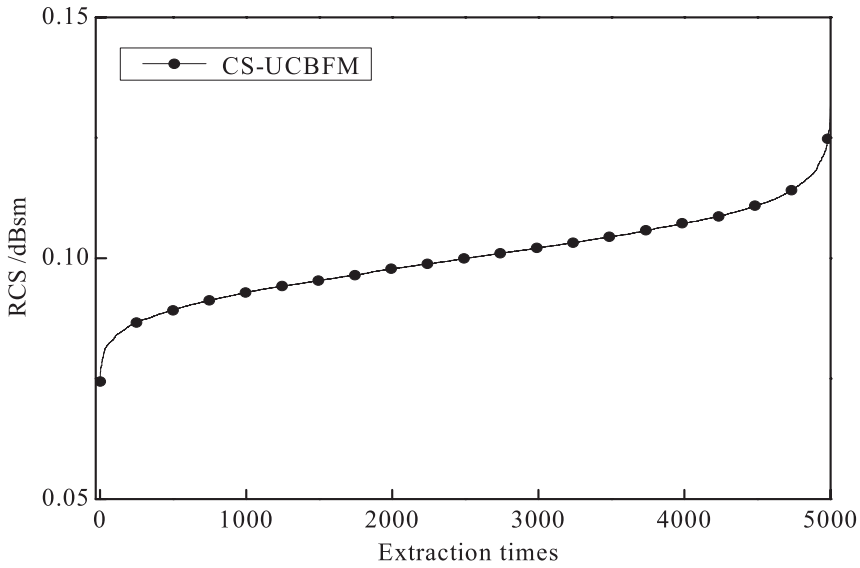

Figure 4. RCS error distribution of 5000 experiments.

by 0.15λ. In this case, a total of 1299UCBFs are obtained using the UCBFM. While CS-UCBFM is used, the extraction ratio of the measurement matrix is controlled at 0.5. Fig. 6 shows the numerical results for RCS of 21 frequency points in the desired frequency band, obtained by the two methods. It is obvious that the results of CS-UCBFM agree well with those of UCBFM and FEKO.

4.2. PEC Cylinder

To further validate the accuracy of CS-UCBFM, we also demonstrate the solution of a PEC cylinder in the frequency range of 0.1G to 2G. The cylindrical geometry has a base radius of 0.12 m and a height of 0.6 m. The geometry is divided into 10 blocks, and each block is extended by 0.15λ in all directions, leading to 22322 unknowns. Here, 1603 UCBFs are obtained by using UCBFM. In this example, the extraction rate of CS-UCBFM is chosen to be 0.3. The numerical results of the wideband RCS for

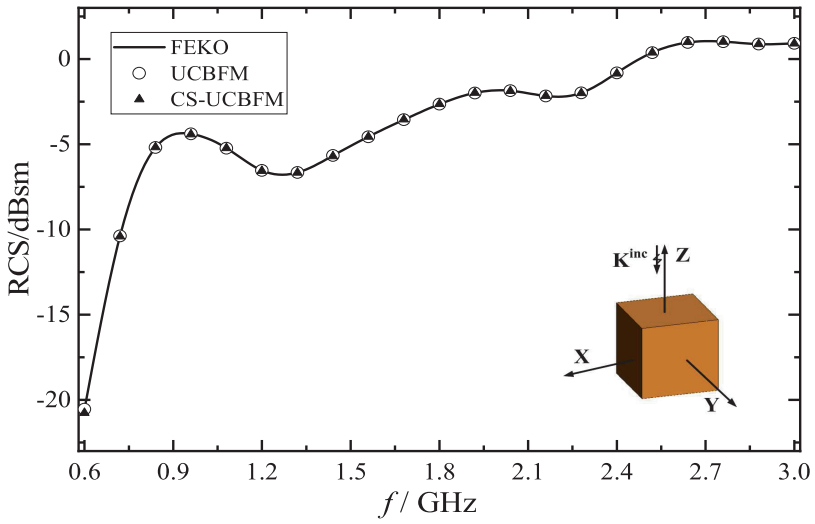

Figure 5. Wideband RCS of the PEC cube.

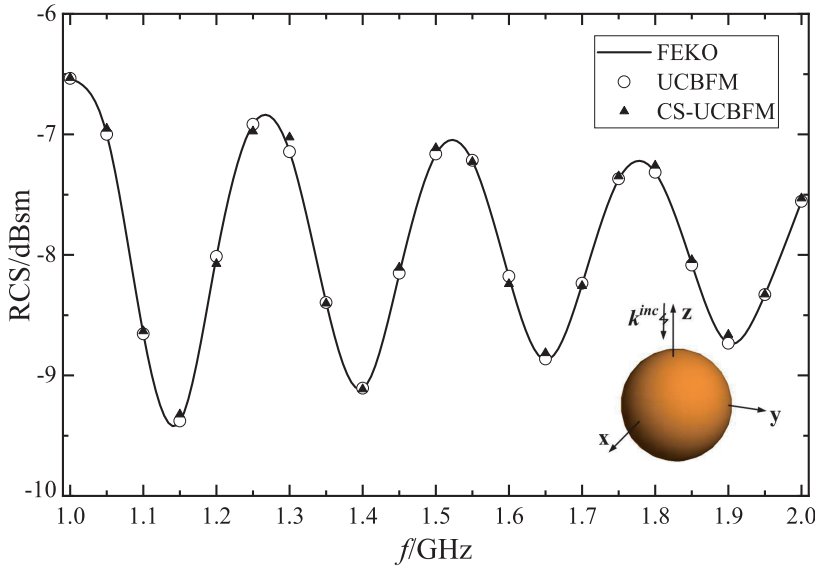

Figure 6. Wideband RCS of the PEC sphere.

21 frequency sampling points calculated using the two methods are shown in Fig. 7. Evident from the figure, the results calculated with CS-UCBFM are in good agreement with those calculated with UCBFM.

Finally, the relevant computation times and RCS errors for the three simulation examples above are given in Table 1. Notably, the construction time of UCBFs includes the filling time of self-impedance matrix at the highest frequency point, and the impedance matrix filling time refers to the average impedance matrix calculation time for all sampling frequency points in the corresponding frequency band. It can be seen that the impedance matrix filling time and RCS solving time of the CS-UCBFM are significantly lower than the UCBFM. Since only a part of the impedance matrix is calculated in the CS-UCBFM, the total time for these three simulations is reduced by 66%, 44%, and 72%, respectively, compared to UCBFM. In addition, as shown in the last column of Table 1, although the error of CS-UCBFM is slightly larger than that of UCBFM, it is still within the acceptable range.

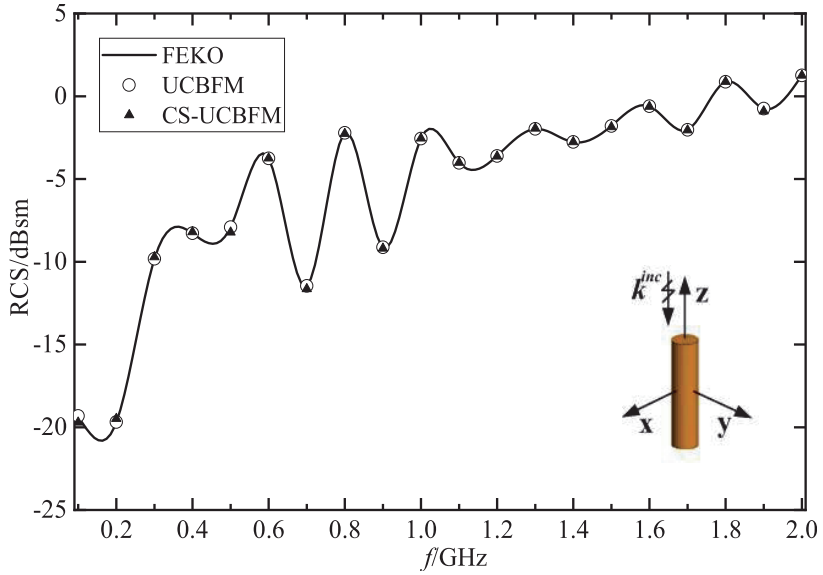

Figure 7. Wideband RCS of the PEC cylinder.

Table 1. Comparison of computation time and RCS error.

Model	Method	UCBFs construction time (s)	Impedance matrix filling time (s)	Average RCS solving time (s)	Total time (s)	RCS Err (%)
Cube	UCBFM	832.9	1097.8	130.7	26631.4	0.092
	CS-UCBFM	826.0	314.1	72.5	8944.6	0.760
Sphere	UCBFM	1670.5	2181.0	325.4	54304.9	0.057
	CS-UCBFM	1654.7	1105.4	271.9	30578.0	0.619
Cylinder	UCBFM	1620.2	2301.3	296.7	53580.2	0.097
	CS-UCBFM	1617.7	512.9	155.2	14979.7	1.704

5. CONCLUSION

In this paper, an effective method combining CS technique and UCBFM is proposed to rapidly solve the wideband electromagnetic scattering problems of target. First, by introducing the domain decomposition strategy, the UCBFs obtained from the self-impedance matrix at the highest frequency point are applied as the sparse basis. Then, CS technique is employed to reduce the number of rows to be filled in the impedance matrix, and an underdetermined equation with small size is constructed based on the sparse basis, thereby reducing the overall computation time. Finally, the induced current is efficiently reconstructed using the least square method. The theoretical analysis and numerical results reveal that the method proposed in this paper can achieve a higher efficiency than the UCBFM, while ensuring sufficient accuracy of wideband RCS calculation.

ACKNOWLEDGMENT

This work was supported in part by the National Natural Science Foundation of China under Grant No. 62071004, in part by the Anhui Provincial Natural Science Foundation of China under Grant

2108085MF200, in part by the Natural Science Foundation of Anhui Provincial Education Department under Grant No. KJ2020A0307, and the Graduate Innovation Fund of Anhui University of Science and Technology under grant No. 2022CX2083.

REFERENCES

1. Coifman, C. R. and V. Rokhlin, "The fast multipole method for the wave equation: A pedestrian prescription," *IEEE Antennas Propag. Mag.*, Vol. 35, No. 3, 7–12, Jun. 1993.
2. Zhao, K., M. N. Vouvakis, and J. F. Lee, "The adaptive cross approximation algorithm for accelerated MoM computations of EMC problems," *IEEE Transactions on Electromagnetic Compatibility*, Vol. 47, No. 4, 763–773, 2005.
3. Chen, X., C. Gu, Z. Niu, and Z. Li, "A hybrid fast dipole method and adaptive modified characteristic basis function method for electromagnetic scattering from perfect electric conducting targets," *Journal of Electromagnetic Waves and Applications*, Vol. 25, No. 14, 1940–1952, 2011.
4. Shaeffer, J., "Direct solve of electrically large integral equations for problem sizes to 1 M unknowns," *IEEE Transactions on Antennas and Propagation*, Vol. 56, No. 8, 2306–2313, 2008.
5. Freni, A., P. De Vita, P. Pirinoli, L. Matekovits, and G. Vecchi, "Fast-factorization acceleration of MoM compressive domain-decomposition," *IEEE Transactions on Antennas and Propagation*, Vol. 59, No. 12, 4588–4599, 2011.
6. Lucente, E., A. Monorchio, and R. Mittra, "An iteration free MoM approach based on excitation independent characteristic basis functions for solving large multiscale electromagnetic scattering problems," *IEEE Transactions on Antennas and Propagation*, Vol. 56, No. 4, 999–1007, 2008.
7. Prakash, V. V. S. and R. Mittra, "Characteristic basis function method: a new technique for efficient solution of method of moments matrix equations," *Microwave and Optical Technology Letters*, Vol. 36, No. 2, 95–100, 2003.
8. Hay, S. G., J. D. O'Sullivan, and R. Mittra, "Connected patch array analysis using the characteristic basis function method," *IEEE Transactions on Antennas and Propagation*, Vol. 59, No. 6, 1828–1837, 2011.
9. Burke, G. J., "Using model based parameter estimation to increase the efficiency of computing electromagnetic transfer functions," *IEEE Trans. Mag.*, Vol. 25, No. 4, 2807–2809, 1988.
10. Newman, E. H., "Generation of wide band from the method of moments by interpolating the impedance matrix," *IEEE Transactions on Antennas and Propagation*, Vol. 36, No. 12, 1820–1824, 1988.
11. Reddy, C. J., M. D. Deshpande, and C. R. Cockrell, "Fast RCS computation over a frequency band using method of moments in conjunction with asymptotic evaluation technique," *IEEE Transactions on Antennas and Propagation*, Vol. 46, No. 8, 1229–1233, 1998.
12. Degiorgi, M., G. Tiberi, and A. Monorchio, "Solution of wide band scattering problems using the characteristic basis function method," *IET Microwaves Antennas and Propagation*, Vol. 6, No. 1, 60–66, 2012.
13. Nie, W. Y. and Z. G. Wang, "Solution for wide band scattering problems by using the improved ultra-wide band characteristic basis function method," *Progress In Electromagnetics Research Letters*, Vol. 58, 37–43, 2016.
14. Nie, W. Y. and Z. G. Wang, "Analysis of wide band scattering from objects using the adaptive improved ultra-wide band characteristic basis functions," *Progress In Electromagnetics Research Letters*, Vol. 60, 45–51, 2016.
15. Yao, A. M., W. Wu, J. Hu, and D. G. Fang, "Combination of ultra-wide band characteristic basis function method and improved adaptive model-based parameter estimation in MoM solution," *2013 Proceedings of the International Symposium on Antennas & Propagation*, 55–58, 2013.
16. Yao, A. M., W. Wu, J. Hu, and D.-G. Fang, "Combination of ultra-wide band characteristic basis function method and asymptotic waveform evaluation method in mom solution," *2013 Proceedings of the International Symposium on Antennas & Propagation*, 795–798, 2013.

17. Chen, M. S., F. L. Liu, H. M. Du, and X. L. Wu, "Compressive sensing for fast analysis of wide-angle monostatic scattering problems," *IEEE Antennas and Wireless Propagation Letters*, Vol. 10, 1243–1246, 2011.
18. Cao, X., M. Chen, X. Wu, M. Kong, J. Hu, and Y. Zhu, "Dual compressed sensing method for solving electromagnetic scattering problems by method of moments," *IEEE Antennas and Wireless Propagation Letters*, Vol. 17, No. 2, 267–270, 2018.
19. Chen, M. S., F. L. Liu, H. M. Du, and X. L. Wu, "Compressive sensing for fast analysis of wide-angle monostatic scattering problems," *IEEE Antennas and Wireless Propagation Letters*, Vol. 10, 1243–1246, 2011.
20. Miosso, C. J., R. von Borries, M. Argaez, L. Velazquez, C. Quintero, and C. M. Potes, "Compressive sensing reconstruction with prior information by iteratively reweighted least-squares," *IEEE Transactions on Signal Processing*, Vol. 57, No. 6, 2424–2431, 2009.